CORE MELT PROGRESSION AND THE ATTAINMENT OF A PERMANENTLY COOLABLE STATE

Robert E. Henry and Hans K. Fauske

Fauske and Associates, Inc.
627 Executive Drive
Willowbrook, Illinois 60521

ABSTRACT

Assessments of the consequences for postulated severe accident conditions in nuclear power plants require a first principle evaluation of the major phenomena associated with overheating of a nuclear core. Three areas essentially govern the containment response since they represent potential containment failure modes: 1) hydrogen production and release from the primary system, 2) steam overpressure as a result of extensive contact between overheated core debris and water, and 3) the coolability of debris in the presence of a continual water supply. These are addressed for typical BWR and PWR primary system and containment configurations, the details of which can have dominant effects on the accident progression/regression. In addition processes are analyzed in which strong competitive phenomena could be occurring such as quenching and oxidation. These are also greatly influenced by the design and accident specific conditions. Finally, the assessment of a permanently coolable state is outlined for various general conditions and the influence of specific design features for BWR and PWR systems is discussed with respect to the variety of accident scenarios that have been considered.

INTRODUCTION

Assessments of postulated severe accident scenarios in a light water reactor involve evaluations of several phenomena within the primary system and the containment; the combined result of which eventually lead to either a permanently coolable state for the once overheated core debris or failure of the containment building. The attainment of a permanently coolable state can be achieved either within the reactor pressure vessel or in the

containment. However, the attainment of such a state requires the continual availability of water to the core debris.

In assessing the accident accommodation, one must consider both the basic features of the primary system as well as the specific geometry and system capabilities of the containment building. These must be considered with respect to the principle phenomena of 1) hydrogen production and the potential for combustion, 2) steam overpressure as a result of quenching and long term cooling for degraded core debris, and 3) the long term coolability of the core material, particularly in an ex-vessel state. In formulating first principle arguments for these phenomena, it is important to consider the specific design characteristics of the systems in question, and the influence these can have on the progression/regression of a given accident. Also, the consequence assessment of postulated severe accidents involves the evaluation of a wide spectrum of accident sequences, and the differences in the reactor states for these sequences must also be included in the evaluation.

STEAM GENERATION

For a postulated state of overheated core debris, the migration of this material into either the lower plenum of the RPV or the containment building could result in contact between the corium and water. Quenching of the core debris would ensue and the steam formed would accumulate in either the primary system or the containment building. In previous computer models, the rate of quenching has been calculated by assuming a particle size to characterize the core debris and the resultant energy transfer rate is governed by internal conduction within the corium particle. In these prior analyses,[1] the particle size assigned to the core debris typically had a radius of a few millimeters. Since the thermal conduction response time (τ) of a particle can be characterized by ($\tau = x^2/\alpha$) ($x = r/3$ for spheres), the calculated time for quenching can be very short. For instance, a corium particle 6 mm in diameter would quench in about 1.3 secs. Such quenching rates for a large number of particles are far in excess of those characterizing the hydrodynamic stability limits for water in the presence of the horizontally heated surface as represented by a saturated pool boiling CHF model.[2,3] This heat flux can be expressed by the Kutateladze equation.

$$q/A = 0.14\, h_{fg} \sqrt{\rho_g} \sqrt[4]{g\sigma_l(\rho_f - \rho_g}} \qquad (1)$$

This is a bi-valued function with respect to pressure, reaching a maximum of 4.3 Mw/m^2 at approximately 7 MPa. If the degraded core material is assumed to be accumulated within the lower plenum of the reactor vessel, the quenching rate from this material would be limited by the ability of the overlying water to remain in contact with the degraded core debris. The critical heat flux expression can be combined with the cross-sectional area of the reactor vessel to determine the maximum steam formation rate. For a typical PWR vessel, this area would be 15 m^2 and at a pressure of 7 MPa, which corresponds to the maximum critical heat flux condition, the resulting steaming rate would be about 60 Mw, or about 2% of the nominal power for a 1000 Mwe plant. However, the point of greatest interest for potential failure of

primary system components is the steam formation rate at the lift pressure of the safety valves (≈ 17 MPa). At this pressure, the critical heat flux is approximately 2.5 Mw/m^2 or a steaming rate of 37.5 Mw. A typical safety valve for a PWR has a capacity of ≈ 45 Mw at the lift pressure and depending upon the system, there may be 2 or 3 such valves on the pressurizer in addition to the PORVs. Consequently, the steaming rates resulting from a quench would be well within the design limits of the safety valves.

For BWRs, the available surface area is more difficult to define because of the CRD tubes which pass through the lower plenum and act as the core support structure. These control rod guide tubes isolate the sealing water for the control rod drive system from that in the reactor coolant inlet plenum region. If the cross-sectional area of the vessel is used as a conservative estimate (≈ 29 m^2) the maximum steaming rate would be about 120 Mw. However, BWR systems are capable of relieving 100% power (∿ 3000 Mw) through their safety relief valves, i.e. such a rapid steam formation would not pressurize the RPV above the SRV set pressure.

This coolant hydrodynamic stability limit can be used to evaluate fragmentation scale during the quench process. Fragmentation determines the surface area available for energy transfer and the resulting heat flux to the water for producing steam. Various models have been proposed in the LMFBR literature for fine scale fragmentation of molten uranium dioxide in direct contact with liquid sodium.[4] For such systems, direct contact is not only possible, but may be sustained for several milliseconds, tens of milliseconds, or longer, since the contact interface temperature is well below the spontaneous nucleation temperature. For a corium-water system the contact interface temperature is several times the thermodynamic critical point of water, and such contacts would result in a local vapor blanketing. As a result, these direct contact mechanisms are not applicable, and the experimental data[5,6] show that the measured fragmentation in non-explosive systems is of a much larger size. Since these corium-water experiments did not observe an explosive interaction and liquid-liquid contact did not occur, this fragmentation process must have occurred under comparative benign hydrodynamic conditions while the material was molten and in the film boiling mode.

For material to accomplish fragmentation in film boiling, a configuration such as that shown in Fig. 1 must be achieved and sustained. If this configuration breaks down by driving water away from molten globules, molten material could coalesce back into larger particles and the fragmentation process would be reversed. Therefore, we can equate the heat flux produced in film boiling to the ability of the water to alleviate such an imposed steam flux, i.e. the pool boiling critical heat flux [Eq. (1)] multiplied by the vessel cross-sectional area. If the water is subcooled, the critical heat flux is increased and can be represented by the subcooled pool boiling critical heat flux correlation of Ivey and Morris:[7]

$$q/A)_{CHF,sub} = \left[1 + 0.1\left(\frac{\rho_g}{\rho_\ell}\right)^{1/4} \frac{c_\ell \rho_\ell \Delta T_{sub}}{\rho_g h_{fg}}\right] q/A)_{CHF,sat} \qquad (2)$$

The film boiling energy transfer for a single particle in film boiling can

be expressed by

$$q_p = 4\pi r_p^2 \left[\sigma\varepsilon(T_F^4 - T_\ell^4) + h(T_F - T_\ell)\right] \tag{3}$$

Given the mass of the molten material, the number of particles and the average fragment radius can be related by

$$n = \frac{3m_T}{4\,\rho_F\,\pi r_p^3} \tag{4}$$

Since the total energy transfer is the sum of the individual contributions

$$q = n\,q_p \tag{5}$$

the total can be expressed by

$$q = \frac{3m_T}{\rho_F r_p}\left[\sigma\varepsilon(T_F^4 - T_\ell^4) + h(T_F - T_\ell)\right] \tag{6}$$

Equating this to the product of the pool boiling CHF and the total cross-sectional area yields

$$r_p = \frac{3m_T\left[\sigma(T_F^4 - T_\ell^4) + h(T_F - T_\ell)\right]}{\rho_F \cdot q/A)_{CHF,sub} \cdot A_v} \tag{7}$$

In this final expression, the emissivity of the water surface has been assumed equal to unity.

This prediction can be compared to the stainless steel and molten uranium dioxide data reported by Benz, et.al.,[5] which shows particle size data from 2 mm up to diameters greater than 4 mm. Typical experimental conditions for these experiments are given in Table I along with the predictions from Eq. (7). In general, this hydrodynamic stability self-limiting mechanism, provides a good characterization of the data over a wide range of experimental conditions.

The data for test runs 28, 39 and 79 were obtained in a large water tank with a coolant to melt volume ratio of 1000:1. In another set of experiments, the authors poured similar quantities of melt into a smaller vessel with coolant-melt volume ratios between 5:1 and 2:1. In this experimental configuration, called a PWR scaled down vessel, the fragment sizes were not reported, but the authors did state, "...in the small tank the melt has been collected on the bottom as a large lump...", and again in discussing the stainless steel results in the smaller vessel, "...the less fragmented melt, which has been collected again as a large lump on the bottom of the vessel." This indicates that the fragmentation was considerably less for the smaller vessel. Carrying out Eq. (7) for the smaller diameter configuration results in a larger fragment size of about 1.4 cm as shown in

Table I, which is consistent with the experimental observations.

Table I

Predicted Melt Fragmentation for the Data of Benz, et.al.

Run	28	39	79	82
Material	SS	SS	UO_2	SS
Melt Temperature, °C	1725	1755	3000	1685
Mass, kg	1.65	2.6	1.24	1.74
Water Temperature, °C	80	20	20	25
Ambient Pressure, MPa	0.1	0.015	0.1	0.1
Tank Volume, m^3	0.2	0.2	0.2	0.0065
$q/A)_{CHF,sat}$, kw/m^2	1187	534	1187	1187
$q/A)_{CHF,SUB}$, kw/m^2	2330	3740	5750	5500
Predicted Particle Diameter, mm	2.8	3.0	5.0	14
Time to Freeze surface, secs	0.36	0.44	-	0.9
Predicted H_2 Generation, kg moles	0.0026	0.0010	-	0.0014
Predicted H_2 Partial Pressure, MPa	0.05	0.016	-	0.83
Measured H_2 Partial Pressure, MPa	0.02	0.013	-	0.70

If this analysis is applied to a reactor accident scenario in which 50% of the core material is assumed to fall into the lower plenum, the fragmentation limit for typical BWR and PWR geometries is given in Table II. As

Table II

Predicted Fragmentation Limits for Hypothetical Accident Conditions in Light Water Reactors

	BWR	PWR
Melt Temperature °C	2,200	2,200
Water Temperature °C	120	285
Mass kg	100,000	50,000
Vessel Area m^2	29	15
Particle Diameter mm	5,200	1,860
Number of Particles	< 1	2

shown the particle sizes are enormous for such a large amount of very hot material in a small area. Obviously such large particles would not exist, but the calculation demonstrates (by orders of magnitude) that in a reactor

system water cannot remain in the presence of fine particulation. As a result, the finely dispersed configurations in intimate contact with water are physically unattainable.

Another feature of the BWR system which also is relevant in assessing the potential for intermixing of molten corium and water is the extensive below core structure. In a BWR the core is supported from below by 185 control rod guide tubes in the latest design. These tubes are 4 m long, about 25 cm in diameter, and are arranged in a square lattice with a pitch of 30 cm. The CRD flow inside these tubes is separated from the inlet plenum water outside the forest of tubes, and except for minor leakage at the inlet to the fuel assembly, these two sources of water do not mix below the top of the core. As a result, the only cross-sectional area available for the intermixing process is that restricted area between the CRD tubes making fragmentation even more difficult than outlined in Table II. In the hypothetical case, the water would be displaced by the downward moving corium and any initiation of fragmentation would only drive the water away faster. It should be noted that only gravity retains the water and that it can readily be displaced into colder (outer) regions of the core, backwards through the jet pumps, etc.

This fragmentation analysis also provides a method of establishing the coarsely intermixed condition envisioned by most steam explosion models. As discussed by Cho, Fauske and Grolmes[8], the minimum amount of energy required to progress from a coarsely intermixed state to a fine scale dispersal can be expressed by:

$$(E_m)_{min} = 1.81\, C_D\, \rho_f\, V \left(\frac{V^{2/3}}{t_m^2}\right)\left(1 - \frac{r^2}{V^{2/3}}\right) \ln\left(\frac{V^{1/3}}{r}\right) \qquad (8)$$

C_D represents the drag coefficient for a dense dispersion of one media moving through another. For typical conditions of interest in these accident evaluations, the volume fractions of the constituents would be essentially equal. Definitive experiments by Rowe[9,10] on the drag forces exerted on an individual particle within a particle bed with about a 40% porosity shows the drag coefficient to be 68 times that of a sphere in an infinite stream, and for equal volume fractions the coefficient is about 20 times the single sphere value. Considering the BWR case for 50% of the core material (100,000 kg) and ignoring the below core structure which would inhibit the mixing as well, the mixing energy required to intimately disperse the 14.3 m^3 volume of corium into an equal volume of water in 0.010 sec (the maximum time interval for an explosive interaction) with a particle size of 1 mm would be 2.2×10^8 kJ. This can be compared with the thermal energy within the 100 tons of debris which is about 1.3×10^8 kJ, i.e. the required mixing energy is of the same order as the thermal energy within the fuel. When this is considered in light of the 1% or less mechanical efficiencies (when compared to the thermal energy) for large scale experiments reported by Buxton, et.al.,[11] the necessary trigger would require about 100 times the work of the explosion itself. If we consider the hypothetical PWR case with 50% of the core (50,000 kg), the fragmentation in film boiling would yield particles 1.86 m in diameter and the energy required to mix down to a size of 1 mm would be 0.17×10^8 kJ as compared to 0.3×10^8 kJ, i.e. the mixing

requirement is again about the same as the thermal energy within the corium. Again considering the experimental efficiencies, the necessary trigger would have to be about two orders of magnitude larger than the scale of the explosion itself. Such "triggers" would not exist within the reactor system for core melt conditions, neither would such a fine scale, intimate dispersal.

As part of this discussion, it should be noted that the aluminum-water steam explosion experiments reported by Long[12] demonstrated the influence of fine particulation in preventing explosive events. In these tests, a reproducibly explosive configuration of a molten stream of aluminum at 750°C, poured through an opening 8.3 cm in diameter, into a square steel container 30.5 cm on a side, filled with water at 20°C was altered by placing a square steel grid over the container. These grid openings where approximately 2.5 cm on side and had the effect of completely eliminating explosive events. Consequently, fine fragmentation has the potential for eliminating the necessary coarse mixing and preventing explosive interactions. In another test series Long increased the drop height from 45.7 cm to 305 cm without the steel grid in place and found that this also eliminated explosions. The reason proposed for this in Ref. [12] is related to the breakup of the aluminum stream: "It appears probable that this high drop broke up the metal stream before it entered the water." This is consistent with the results with the steel grid and the analysis presented above. The detailed results of Long's experiments are analyzed in light of this film boiling fragmentation mechanism in Ref. [13].

In summary, if molten corium material falls into water, the initial configuration would be film boiling, and the fragmentation would be a self-limiting process governed by the hydrodynamic stability of the water. This results in very large particle sizes for both reactor systems, and as a result the maximum steam formation rate is well below the overpressure relief capacity of both systems. Given this fragmentation level, the energy required to rapidly mix the two materials (to produce a large scale steam explosion) is orders of magnitude greater than that typically produced by such events, i.e. large scale steam explosions involving significant quantities of fuel could not occur and are not a viable containment failure mechanism.

HYDROGEN GENERATION

Light water reactors are in their most reactive configuration during the normal operation of the power plant. For the accident sequences considered, the reactor itself is shutdown. As a result, core damage only occurs with a loss of water inventory from the primary system. This loss can be postulated to result from a break in the primary system (large and small break loss of coolant accidents) or a loss of heat removal capabilities from the primary system. Depending upon the accident sequence, the rate of uncovery for the nuclear core is on a time scale from minutes to hours and essentially occurs in the absence of strong hydrodynamic forces since such forces would be the result of coolant flow which would easily provide cooling for the core at these decay power levels. As has been discussed for the TMI-2 accident[14] the boil-down of the water level allowed the cladding

to overheat such that oxidation could occur at a significant rate. Estimates of this process have calculated approximately 50%[15] of the zircaloy cladding within the TMI-2 core could have been oxidized. Several key features of the intact geometrical configuration would substantially affect the process, as compared to continued oxidation after the intact geometry is lost.

1. In this configuration, the zircaloy cladding and the uranium dioxide fuel are separated and the zircaloy is in direct contact with the coolant.

2. The zircaloy has only been heated to temperatures typical of normal operation and as a result the oxide layer on the surface is of only minimal thickness.

3. The cladding is heated from within by the decay power generated within the fuel pellets and the overheating process occurs over tens of minutes.

4. The steam flow is in direct contact with the overheated cladding and the oxidation rate is governed only by the oxidation history of the cladding and the availability of oxygen to the cladding surface.

5. The net process is one of increasing the temperature of the cladding and this is further driven by the autocatalytic affect of the exothermic reaction resulting from zircaloy oxidation. This further increase in the temperature accelerates the reaction rate.

This oxidation process in the original core configuration is to be contrasted with those processes envisioned when a mixture of molten core material moves outside of the core boundaries and into the lower plenum of the reactor vessel or into the containment building. Like the steam formation rate discussed above, for many analyses conducted to date, the oxidation outside the core boundaries has been assumed to be efficient in terms of reacting the remaining metallic zircaloy. In this configuration, the process of quenching and further oxidation are competitive rate dependent processes since the quenching of the core debris acts to reduce the temperature of the degraded material and sustained oxidation requires that the temperature remains at an elevated level for the reaction to continue. As a result, it is unrealistic to assume that both processes go to completion. In general, the temperatures considered for the degraded core material in these processes outside the original core boundaries are those typical of a molten state which would be 2500°K or greater. As discussed in the previous section, the principle means of energy transfer during an interaction between water and the core material would be thermal radiation and the size of the fragments, and thus the particulate surface area, is limited by the ability to retain water in the immediate vicinity of the molten material. This is also a basic configuration necessary for sustained oxidation, since the water supplies the steam which in turn supplies the oxygen for continued oxidation. If the fragmentation processes attempts to generate the fine scale intermixing configuration, the steam formed by film boiling alone is sufficient to displace the water and allow the particles to coalesce back into a larger size. Given a molten fragmented state, the oxidation process can be estimated based upon the ability to diffuse hydrogen away from the

heated surface and thereby allow steam to diffuse into the surface to sustain the oxidation process. For such a mechanism, the molar flux of hydrogen diffusion can be estimated from

$$N/A = \frac{D_v}{RT} \frac{(P_{g,s} - P_g)}{\delta_s} \tag{9}$$

The gas-vapor layer thickness (δ_g) can be estimated from the convective film boiling heat transfer coefficient and the steam thermal conductivity

$$\delta_s = k_s/h \tag{10}$$

A typical value at low pressures for h would be 0.3 kw/m^2 sec°C which yields a layer thickness of 80 μm.

In the experiments of Benz, et.al.,[5] molten stainless steel, heated in an inert environment was poured into water. After the quenching of the debris was complete, the pressure in the test vessel was greater than before the experiment, reflecting the formation of a non-condensible gas, i.e. H_2. As discussed in Section II, the particle diameter determined by the film boiling, hydrodynamic stability is a few millimeters. Given this surface area, one only has to know the time interval over which the diffusion model is applicable. In these estimative calculations this is set equal to the lesser of the time to cool the entire particle to the solidification point or the time at which the thermal conduction to the surface cannot supply the radiative heat flux. The first time can be easily estimated by considering only the radiative heat flux

$$-\rho_F(4/3\ \pi\ r_p^3)c_F \frac{dT_F}{d\theta} = \sigma T_F^4 \tag{11}$$

which can be integrated to

$$\theta = \frac{\rho_F r_p c_F}{9\sigma} \left[\frac{1}{T_{F,m}^3} - \frac{1}{T_F^3}\right] \tag{12}$$

The second time interval, which is generally applicable to large particles can be estimated from the error function solution

$$\theta = \frac{1}{\pi \alpha_F} \left\{\frac{k_F(T_F - T_{F,m})}{\sigma\ T_F^4}\right\}^2 \tag{13}$$

These times approximate the interval until the surface and sublayers would freeze thus requiring the oxidation to be sustained by diffusion through the solid layer which is a much slower process than a process which is only limited by H_2 diffusion through a gaseous layer. The calculated time intervals ignore internal circulation, but the times are so short that these motions would have little influence on the heat flux. In addition corium

becomes viscous in the vicinity of the liquidus point which would minimize any circulation near the surface.

Table I lists a comparison of the predicted and measured H_2 generation for the experiments carried out by Benz, et.al.[5] The agreement is quite good considering the ranges of system pressure, water subcooling, and fragment size. These tests were performed with unreacted-stainless steel which is much different than the reactor system in which about 80% of the material is UO_2 and the remainder is a combination of metallic zircaloy and stainless steel and their respective oxides, i.e. the corium mixture is already mostly composed of oxide materials. As a result, calculating the H_2 evolution based upon a gaseous layer diffusion model is highly conservative. However, carrying out such calculations a BWR results in surface freezing in 2 secs, and for 100 tons of material with a surface area of 28.5 m^2, the amount of H_2 generated would be 1.7 kg moles which represents an oxidation of approximately 0.1%, i.e. a very small amount of additional oxidation even using this conservative calculation. Carrying out such calculations for the higher pressure PWR accident case, used as a reference herein, results in an additional oxidation of about 7% of the core material, this value principally being greater because of the higher pressure used in the accident sequence.

In summary, the film boiling fragmentation model provides an estimate of the available surface area for continued H_2 formation. A conservative gas layer diffusion model bounds data taken for a pure metallic system, and when this approach is applied to a reactor system, which would greatly overestimate the H_2 evolution, the additional amount of H_2 generated is a small increment to that produced in the original core configuration such as that determined for TMI. Therefore, the additional H_2 generated during quenching processes is a very small amount and well within the uncertainties generally assigned to that generated when the geometry is intact.

DEBRIS BED COOLABILITY

This issue is relevant to both in-vessel termination of an accident and to the establishment of a stable ex-vessel state, and in both cases the necessary requirement is a continual supply of water to the damaged core material. The particular issues to be addressed are the fragmented size of the debris in this quenched configuration and the ability of water to permeate the fragmented geometry so that a substained coolable condition is achieved. Several models have been proposed to describe the limit of coolability for debris bed configurations such as the annular flow model proposed by Harden and Nielson,[15] the correlation proposed by Dhir and Catton[16] to describe the limit for the ability of water to permeate to the bottom of the debris bed, the counter flow liquid-vapor model proposed by Lipinski[17] wherein each particle is covered by a liquid film and vapor is passing upward between the particles, and the laminar flow model proposed by Jones, et.al.[18] These models all describe the limit of coolability for particle beds as a function of the bed porosity and particle diameter.

It is proposed here that dryout within a coarse ($d > 1$ mm) particulate bed coincides with the onset of fluidization of the water either within the

upper portion of the bed or at the upper surface. This point can be determined by considering liquid droplets whose diameter is that of the particles and the vapor channels are separated by the same dimension. A force balance determines the fluidization point (the drag force equals the weight).

$$u_F^2 = \frac{4g}{3C_D} \frac{\rho_f}{\rho_g} d \tag{14}$$

The dryout heat flux is then simply given by

$$q/A)_{DO} = h_{fg} \rho_g \sqrt{\frac{4g}{3C_D} \frac{\rho_f}{\rho_g} d} \tag{15}$$

As discussed in Section II, for solid spherical particles C_D has been shown by Rowe, et.al.[15,16] to be 68.5 times larger than the drag coefficient for a single particle in an infinite sea ($C_D \sim 1.0$). A similar value of C_D would be expected for fluidized liquid droplets at the minimum fluidization point ($\alpha = 0.40$).

To further illustrate the point, we shall make use of Kutateladze's classical experiments with the water-mercury system, where mercury was coarsely fragmented by water flowing through the porous plate located below the mercury bath. The sharp transition to a fluidized state occurred for a superficial water velocity given by

$$u = 0.2 \rho_\ell^{-1/2} [\sigma_1 g(\rho_{Hg} - \rho_\ell)]^{1/4} \tag{16}$$

where σ_1 is the surface tension. Equation (16) yields a water velocity of ~ 8.5 cm and since the droplet size is proportional to $\sigma_1/g(\rho_{Hg} - \rho_\ell)$, the diameter can be estimated from

$$\frac{\rho u^2 d}{\sigma} = 0.2^2 \tag{17}$$

yielding a value of ~ 0.28 cm. The volume fraction of water at the point of incipient fluidization [Eq. (16)] is ~ 0.4 and the drag caused by the streaming water must just balance the weight of the mercury droplets, i.e.

$$C_D = \frac{8}{3} \frac{4\rho_{Hg} g}{\rho_\ell u^2} \tag{18}$$

For the droplet laden mixture of mercury in water, the effective drag coefficient is estimated to be ~ 68, in excellent agreement with the value corresponding to fluidization of solid particles at the minimum point.

Using a value of $C_D \sim 68$ in Eq. (15), we obtain the predicted values shown in Fig. 1, and the comparison with the experimental results from Refs. [20,21] and [22] is excellent.

If we now consider the fragmentation scale for the various accident sequences, we can determine if the resultant particle sizes generated in these scenarios would present a configuration capable of removing the decay power, i.e. a stable, coolable state. For instance, if 50% of the core material from a BWR is assumed to be transmitted to a suppression pool with a cross-sectional area of 500 m^2, at a pressure of 0.1 MPa, and a pool temperature of 50°C. Given these parameters, the resulting particle size would have a radius of about 6 cm. Using the particle bed model described above, the limiting heat flux would be about 8.5 Mw/m^2 and the heat removal rate at the hydrodynamic limitation would be over 4000 Mw, i.e. a value much greater than the decay power indicating the bed is permanently coolable.

For smaller cross-sectional areas in the water pool, whether inside the RPV or in a reactor cavity typical of PWR designs, the resulting fragment sizes would be larger and thus even less of a hydrodynamic limitation than discussed above. Consequently, these would also be permanently coolable in the presence of a continual water supply sufficient to remove the decay power. One additional aspect of the smaller geometries of the reactor cavities could be the time required to quench the overheated debris once it is assumed to be released from the RPV. Assuming the quench process to be limited by a saturated CHF and a reactor cavity area of 50 m^2, the quench interval for 50 tons of debris could be as long as 20 mins. Taking the experimental results reported for concrete penetration in the absence of water[23] and using an average attack rate of 1.5 cm/min to represent the total temperature spectrum, the depth of the thermal attack during the quench would be about 15 cm. (The rapid thermal attack only occurs when the corium temperature is above the concrete melting point, assumed to be 1400°K in these estimates.) This would be a negligible depth of attack, and the principal feature of the concrete attack would be the gas evolved. For the agressive thermal attack to progress, this gas must be alleviated upward through the debris. As with the steam flow considered earlier, this flow of non-condensible gases can significantly affect the formation of the debris bed, especially in two key manners: 1) the gas would help fragment the debris to a typical size of a few centimeters, and 2) the upward flowing gas which would be formed at the bottom of the bed could loosen a bed which would begin to become compact with non-spherical particles. This is similar to the film boiling fragmentation model in that it is a self-limiting process, i.e. if no gas is formed the bed is coolable and if the bed is not coolable such that non-condensible gases are formed, the result will be to loosen up the bed and make it more coolable.

CONCLUSIONS

The processes associated with fragmentation, steam formation, hydrogen production, and ultimate coolability have been assessed for typical PWR and BWR accident configurations. First principle analyses demonstrate that fine scale fragmentation with a substantial quantity of debris cannot occur within the RPV and the fragment sizes in an ex-vessel state would be at least several centimeters in diameter. As a result, 1) steam formation rates would be limited to values easily relieved by the primary system safety valves, 2) the maximum amount of H_2 generated after the core leaves the original core boundaries is a small amount compared to that which could

be produced during the heatup phase, and 3) the fragment sizes represent a permanently coolable state in the presence of a sufficient continual water supply.

REFERENCES

1. Reactor Safety Study, WASH-1400, NUREG/750114, 1975.

2. S. S. KUTATELADZE, "Elements of Hydrodynamics of Gas-Liquid Systems," Fluid Mechanics - Soviet Research, Vol. 1, 4, 1972, p. 29.

3. N. ZUBER, "Hydrodynamic Aspects of Boiling Heat Transfer," USAEC, AECU-4439, 1959.

4. A. W. CRONENBERG and M. A. GROLMES, "A Review of Fragmentation Models Relative to Molten UO_2 Breakup When Quenched in Sodium Coolant," Proc. of the Third Specialists Mtg. on Sodium/Fuel Interaction in Fast Reactors, PNC N251 76-12, Vol. 2, March 1976, pp. 623-650.

5. R. BENZ, W. SCHWALBE, H. HOHMANN and F. TOSELLI, "Melt/Water and Reactions in Tank Geometry: Experimental and Theoretical Results," Proc. of the Fourth CSNI Specialist Mtg. on Fuel-Coolant Interaction and Nuclear Reactor Safety, CSNI Report No. 37, Vol. 2, Bournemouth, UK, April 1979, pp. 363-386.

6. M. AMBLARD, et.al., "Experimental Results of Contact Between Molten UO_2 and H_2O: Statement of Thermal Interaction Models," OECD CSNI Specialist Mtg. on the Behavior of Water Reactor Fuel Elements Under Accident Conditions, Spatind, Norway, September 1976.

7. H. J. IVEY and D. J. MORRIS, "On the Relevance of Vapor-Liquid Exchange Mechanism for Subcooled Boiling Heat Transfer High Pressures," AEW-R-137, Winfrith, 1962.

8. D. J. CHO, H. K. FAUSKE and M. A. GROLMES, "Some Aspects of Mixing in Large-Mass, Energetic Fuel-Coolant Interactions," Proc. of the Intl. Mtg. on Fast Reactor Safety and Related Physics, CONS-761001, Vol. 4, Chicago, IL, October 1976, pp. 1852-1861.

9. P. N. ROWE and G. A. HENWOOD, "Drag Forces in a Hydraulic Model of a Fluidized Bed - Part I," Trans. of the Institute of Chemical Engineers, Vol. 39, 1961, pp. 43-54.

10. P. N. ROWE, "Drag Force in a Hydraulic Model of a Fluidized Bed - Part II," Trans. of the Institute of Chemical Engineers, Vol. 39, 1961, pp. 175-180.

11. L. D. BUXTON and W. B. BENEDICK, "Steam Explosion Efficiency Studies," NUREG/CR-0947, SAND-79-1399, November 1979.

12. G. LONG, "Explosions of Molten Aluminum and Water - Cause and Prevention," Metal Prog., May 1957.

13. R. E. HENRY and H. K. FAUSKE, "Required Initial Conditions for Energetic Steam Explosions," paper accepted for presentation at the ASME Winter Annual Mtg., Washington, D.C., November 1981.

14. "Analysis of Three Mile Island-Unit 2 Accident," NSAC-1, July 1979.

15. "Supplement of Analysis of Three Mile Island-Unit 2 Accident," NSAC-1 Supplement, October 1979.

16. H. C. HARDEE and R. H. NIELSON, "Natural Convection and Porous Media with Heat Generation," Nucl. Sci. Eng., Vol. 63, 1977, pp. 119-132.

17. V. K. DHIR and I. CATTON, "Prediction of Dryout Heat Fluxes in Beds of Volumetrically Heated Particles," Proc. of the Intl. Mtg. of Fast Reactor Safety and Related Physics, Chicago, IL, Vol. IV, October 1976, pp. 2026-2035.

18. R. J. LIPINSKI, "A Particle-Bed Dryout Model with Upward and Downward Boiling," Trans. ANS, 36, November 1980, pp. 358-360.

19. S. W. JONES, M. EPSTEIN, J. D. GABOR, J. C. CASSULO and S. G. BANKOFF, "Investigation of Limiting Boiling Heat Fluxes from Debris Beds," Trans. ANS, 35, November 1980, pp. 361-363.

20. L. BARLEON and H. WERLE, "Dependence of Debris Bed Dryout Flux on Particle Diameter," Trans ANS, 38, June 1981, pp. 382-392.

21. R. TRENDBERTH and G. F. STEVENS, "Experimental Study for the Heat Transfer and Dryout in Heated Particulated Bed," AEEW-R1342, July 1980.

22. D. SQUARER, A. T. PIECZYNSKI and L. E. HOCHREITER, "Dryout in Large Particle, Deep Beds," Trans. ANS, 38, June 1981, pp. 444-445.

23. D. A. POWERS, "Molten Stainless Steel/Concrete Interaction Tests," SAND-77-1423, June 1978.

NOMENCLATURE

A - area

A_v - cross-sectional area of the vessel

c_F - specific heat of corium

c_ℓ - specific heat of water

D_v - mass diffusivity of hydrogen

$E_m)_{min}$ - minimum mixing energy

g - acceleration of gravity

h - heat transfer coefficient

$q/A)_{CHF,sub}$ - subcooled critical heat flux

$q/A)_{DO}$ - dryout heat flux

r - radius

r_p - particle radius

T_ℓ - water temperature

T_F - corium temperature

ΔT_{sub} - water subcooling

V - volume

h_{fg} - latent heat of vaporization

k_s - thermal conductivity of steam

m_T - total mass of corium

n - number of particles

N - molar condensation rate

p_g - pressure of the gas space

$p_{g,s}$ - partial pressure of steam

q - energy transfer

q_p - particle energy transfer

q/A - heat flux

$q/A)_{CHF,sat}$ - saturated critical heat flux

x - characteristic length

Greek Symbols

α - thermal diffusivity

δ_s - steam film thickness

ρ_f - saturated water density

ρ_F - corium density

ρ_g - saturated vapor density

ρ_{Hg} - mercury density

ρ_ℓ - subcooled water density

σ - Stefan-Boltzmann constant

σ_1 - liquid-vapor surface tension

τ - time constant

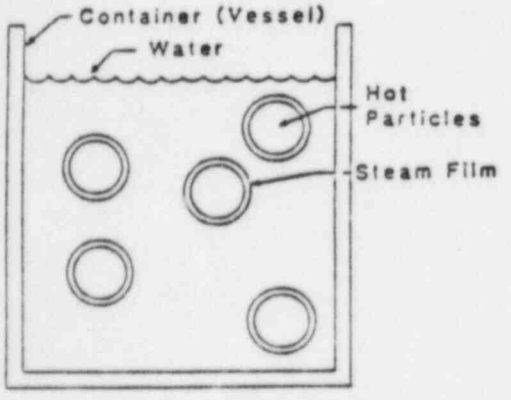

Fig. 1 Film Boiling Fragmentation

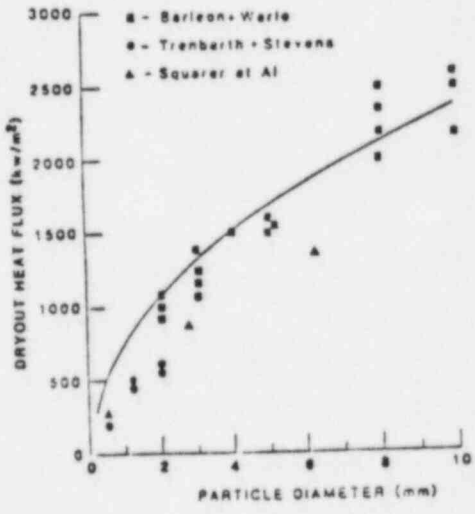

Fig. 2 Comparison of Debris Bed Dryout Model with Experimental Data